Werk

Jahr: 1982
Kollektion: fid.geo
Signatur: 8 Z NAT 2148:51
Digitalisiert: Niedersächsische Staats- und Universitätsbibliothek Göttingen
Werk Id: PPN1015067948_0051
PURL: http://resolver.sub.uni-goettingen.de/purl?PPN1015067948_0051

LOG Id: LOG_0035
LOG Titel: Analysis of broad-band Rayleigh waves: A possibility for seismic discrimination
LOG Typ: article

Übergeordnetes Werk

Werk Id: PPN1015067948
PURL: http://resolver.sub.uni-goettingen.de/purl?PPN1015067948
OPAC: http://opac.sub.uni-goettingen.de/DB=1/PPN?PPN=1015067948

Contact

Niedersächsische Staats- und Universitätsbibliothek Göttingen
Georg-August-Universität Göttingen
Platz der Göttinger Sieben 1
37073 Göttingen
Germany
Email: gdz@sub.uni-goettingen.de

J Geophys (1982) 51:165–179

Journal of Geophysics

Analysis of Broad-Band Rayleigh Waves: A Possibility for Seismic Discrimination

W. Hanka
Bundesanstalt für Geowissenschaften und Rohstoffe, Stilleweg 2, D-3000 Hannover, Federal Republic of Germany

Abstract. Digital broad-band data like those of the Graefenberg (GRF)-Array in Southern Germany offer enhanced possibilities for the investigation of the medium-period band between 2 s and 20 s. This range plays an important role for surface wave studies in particular. Synthetic Rayleigh wave seismograms, computed using the reflectivity method, show that most of the stationary phases for continental travel paths and teleseismic distances appear mainly in this particular range. The influence of source parameters (source depth, source spectrum and source type and orientation) on the excitation of Rayleigh waves for a laterally homogeneous continental earth model is discussed in detail. Differences in the frequency-time diagrams of synthetic Rayleigh waves excited by explosion and dislocation point sources at various depths with different source spectra are also found in recorded seismograms. A quantification of these differences by amplitude ratios in the frequency-time domain leads to discrimination parameters which allow the separation of underground nuclear explosions from earthquakes by an estimation of the source depth or the source spectrum. These parameters are verified for a set of 20 nuclear explosions and 20 earthquakes from the southern USSR and adjacent areas.

Key words: Broad-band Rayleigh waves – Stationary phases – Reflectivity method – Seismic discrimination.

Introduction

Theoretical investigations by Knopoff et al. (1973), Panza and Calcagnile (1975), Schwab et al. (1974), Calcagnile and Panza (1974), Nakanishi et al. (1976), Stephens and Isacks (1977) and Mantovani et al. (1977) explain a number of impulsive seismic phases such as *Rg*, *Lg*, *Li*, *Sa*, *Ma* and *Sn* in terms of stationary or Airy-phases, or superimposed Airy-phases, of fundamental and higher mode Love and Rayleigh waves. These phases are guided by different parts of the earth's interior. The *Rg* and *Lg* phases travel mainly in the upper continental crust ('granitic layer'), the *Sn* phase in the high-velocity 'lid' in the uppermost mantle and the different parts of the *Sa* phase or *Ma* phase (vertical part of *Sa*) sample the mantle structure down to the '400-km-' or '650-km'-discontinuity in a realistic earth model. No low-velocity layer in the crust or the upper mantle is required to explain the group velocity maxima and minima corresponding to these phases. Only the *Li*-phase requires a low-velocity channel in the upper mantle model.

For continental paths and teleseismic distances most of the stationary phases – except the main part of *Sa* (or *Ma*) – appear in the medium-period band between 2 s and 20 s. In particular, the surface waves of Russian nuclear explosions recorded at the GRF-Array have their major signal content in this range. Seismic standard stations, like the WWSSN (World Wide Standard Seismograph Network) and the SRO-stations (Seismic Research Observatory), usually exclude an important part of this band from acquisition because of the appearance of the strong microseismic noise between 4 s and 10 s. With the installation of the Graefenberg (GRF) digital braod-band array in Southern Germany enhanced possibilities for the investigation of the medium-period band are offered (Harjes and Seidl, 1978). This is due to a flat velocity response of the leafspring seismometers (Wielandt, 1975) between 0.05 Hz and 5 Hz.

For seismic discrimination of underground nuclear explosions and earthquakes surface wave information apart from the surface wave magnitude M_s or related values is very little used. Investigations regarding the use of regional *Lg* (or *Sg*) and *Sn* in combination with *Pg* and *Pn* recorded at short-period WWSSN-stations have recently been carried out by Gupta et al. (1980), Nuttli (1981), Gupta and Burnetti (1981) and Mykkeltveit and Husebye (1981) for regional distances ($\Delta < 30°$). The best results for discrimination of regional events, in cases of sufficient *Lg* propagation, were obtained from the *Lg*/*P* ratio (Gupta et al., 1980; Gupta and Burnetti, 1981), and from the (maximum before *Sn*)/(maximum after *Sn*) ratio (Gupta and Burnetti, 1981), where both ratios represent regional equivalents of the teleseismic m_b/M_s criterion. Amplitude ratios of higher mode phases such as *Sn*/*Lg* or *Lg* (early arriving)/*Lg*(late arriving) show no significant differences.

Nuttli (1981), on the other hand, found too large an overlap for the *Lg*/*P* ratio of Russian nuclear explosions and Western and Central Asian earthquakes implying that this is not a useful discriminant for that region. Mykkeltveit and Husebye (1981) also did not receive sufficiently acceptable results using *Lg* or *Sn* amplitudes measured on WWSSN records (SP and LP) for the discrimination of events from the same region. Only the periods of these phases recorded on long-period WWSSN seismometer are different for explosions and earthquakes.

The purpose of this paper is the investigation of the complete teleseismic Rayleigh wave seismogram for conti-

0340-062X/82/0051/0165/$03.00

nental travel paths including all stationary phases in the medium- and long-period band up to 80 s with special regard to the influence of the source parameters on the Rayleigh wave excitation. This study therefore contains model computations as well as the analysis of observed broad-band seismograms. The results will then be quantified and used for the discrimination of actual data.

Computation and Analysis of Synthetic Rayleigh Wave Seismograms

The influence of the various source parameters (source type and orientation, source spectrum and source depth) and the travel path parameters (velocity-depth function, attenuation-depth function and distance) on the excitation of surface waves cannot be estimated by direct inversion of the observed seismogram. Therefore an iterative forward modelling approach is applied using theoretical surface wave seismograms. In this study the influence of source parameters is evaluated for a fixed travel path model and a fixed distance. The computation of synthetic seismograms is carried out using the reflectivity method for a buried source (Kind, 1978, 1979). This method allows computations of complete seismograms including all body and surface waves for laterally homogeneous earth models.

The Aki-model (Aki, 1967) for dislocation sources and the Mueller-Murphy-model (Mueller and Murphy, 1971) for nuclear explosions are used for the evaluation of source spectra. The Aki-spectra for M_s-values of 4, 5 and 6 and the Mueller-Murphy- (MM-) spectrum for a yield of 1 Mt are normalized, transformed into ground velocity and truncated between 0.7 Hz and 0.75 Hz, with is the highest computed frequency (Fig. 1).

The velocity-depth model (Fig. 2) represents the travel path Novaya Zemlya-GRF and is evaluated down to approximately 40 km by the inversion of fundamental mode Rayleigh waves of a presumed nuclear explosion. The travel path consists of a high-velocity part, the Baltic shield, and a low-velocity part, the Barents Sea. Therefore the velocities of the average model are quite low for a continental structure. The upper mantle model is estimated from investigations for Western Europe by Seidl (1971). To reduce computing time the '400-km-discontinuity' is placed at 280 km without serious changes in the shape of the theoretical dispersion curves. The attenuation model used is based on a standard Q-model (SL8) by Anderson and Hart (1978) with a high-Q crust to which low-Q sedimentary layers were added. All seismograms are computed for an epicentral distance of 30°.

A frequency-time-analysis – using the 'multiple-filter-technique' (Dziewonski et al., 1969) – is applied to the synthetic Rayleigh wave seismograms to separate the different modes included in the complex transient wave train. In all cases the period range between 1 s and 80 s and the group velocity window between 5 km/s and 2 km/s is analysed and the results of the upper 42 db of the matrix are plotted in Fig. 3–Fig. 7 in 6-db-contour-intervals. Local maxima in various group velocity intervals are marked by crosses for each period. The computed seismogram is also plotted with the same group velocity scale.

The influence of the different source parameters, as they result from the theoretical investigation, are summarized as follows:

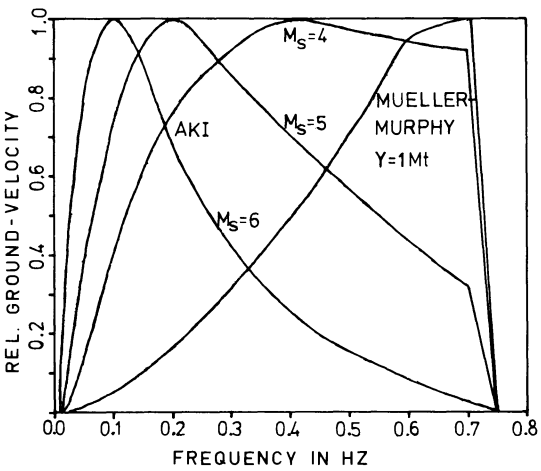

Fig. 1. Source spectra used for computations: earthquake spectra based on the Aki model ($M_s=4$, 5 and 6) and a nuclear explosion spectrum based on the Mueller-Murphy model ($Y=1$ Mt)

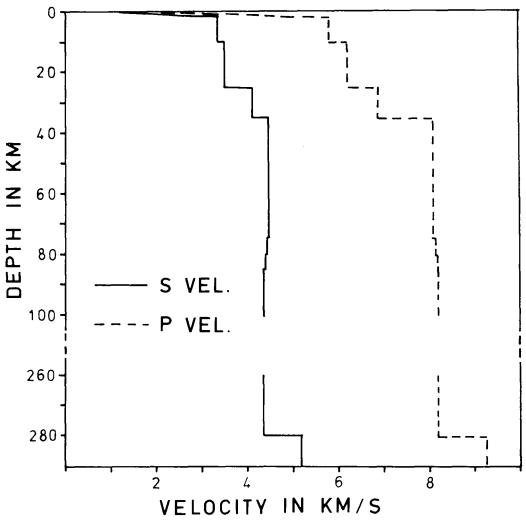

Fig. 2. Velocity-depth model used for computations representing the travel path Novaya Zemlya – GRF

Source Depth

The source depth is varied from 0.3 km to 250 km for an explosion point source with an MM-spectrum ($Y=1$ Mt) in Fig. 3 and a vertical strike-slip point source (slip-angle $\lambda=0°$, dip-angle $\delta=90°$, observation angle $\Theta=45°$) with an Aki-spectrum ($M_s=6$) in Fig. 4. In both cases the source depth is the main factor determining the parts of the dispersion curves of the different modes which are excited. Therefore the excitation maximum is found at that part of the curves which corresponds to the source depth. The periods due to the maximum or other characteristic parts of the seismogram increase with depth.

The crustal phases *Rg* and *Lg* are observed down to a source depth of 40 km and the periods corresponding to the maxima increase with depth. The *Lg*/*Rg* ratio varies according to the different amplitude-depth functions. Starting from 40 km depth the mantle guided phase *Sn*, and from 100 km depth the *Ma* phase, appear as well as the strongly dispersed parts of the first four Rayleigh wave modes. At 250 km depth the stationary parts of the higher

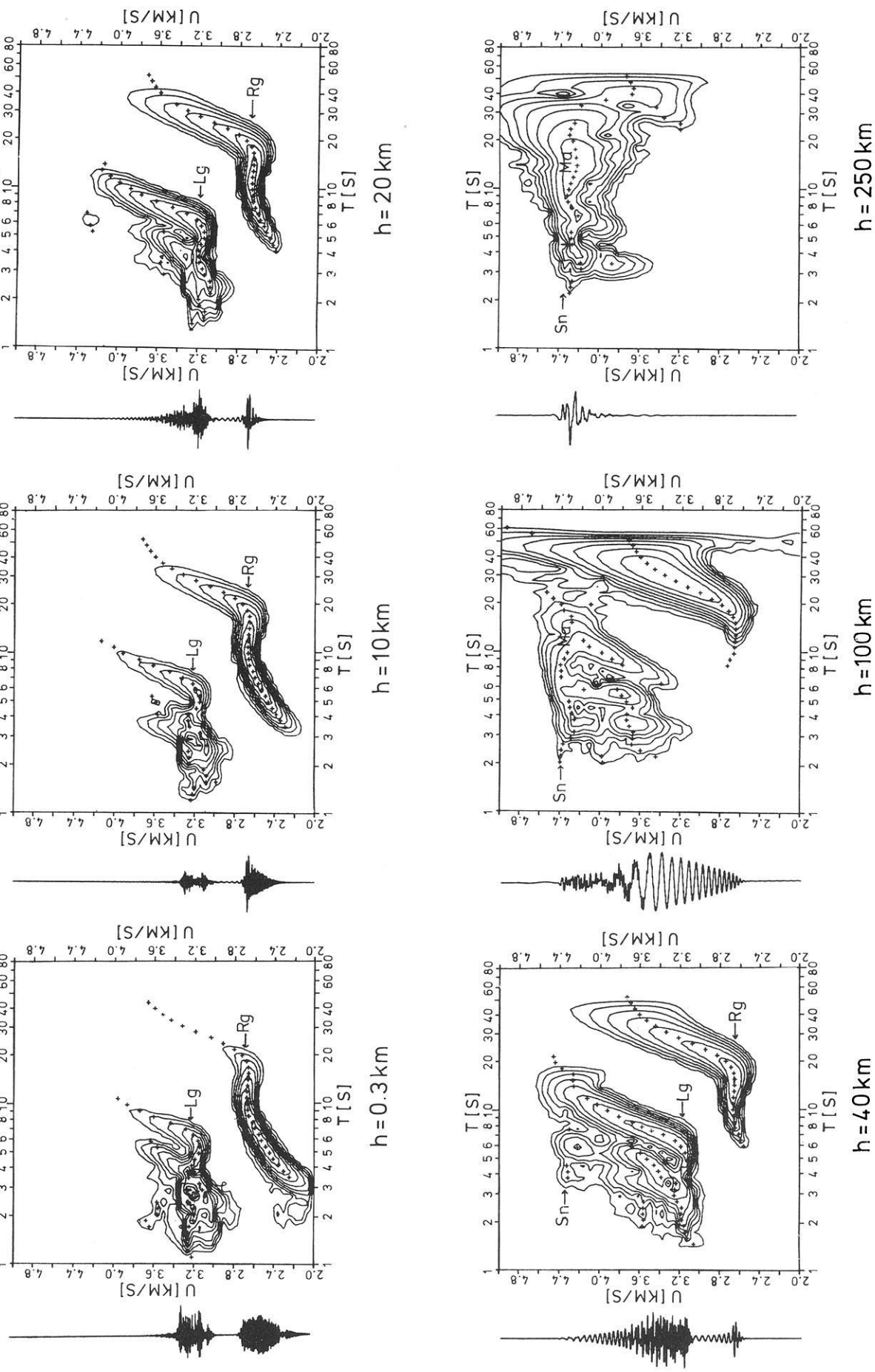

Fig. 3. Depth dependence of the excitation of Rayleigh waves for an explosion point source and a Mueller-Murphy spectrum (1 Mt)

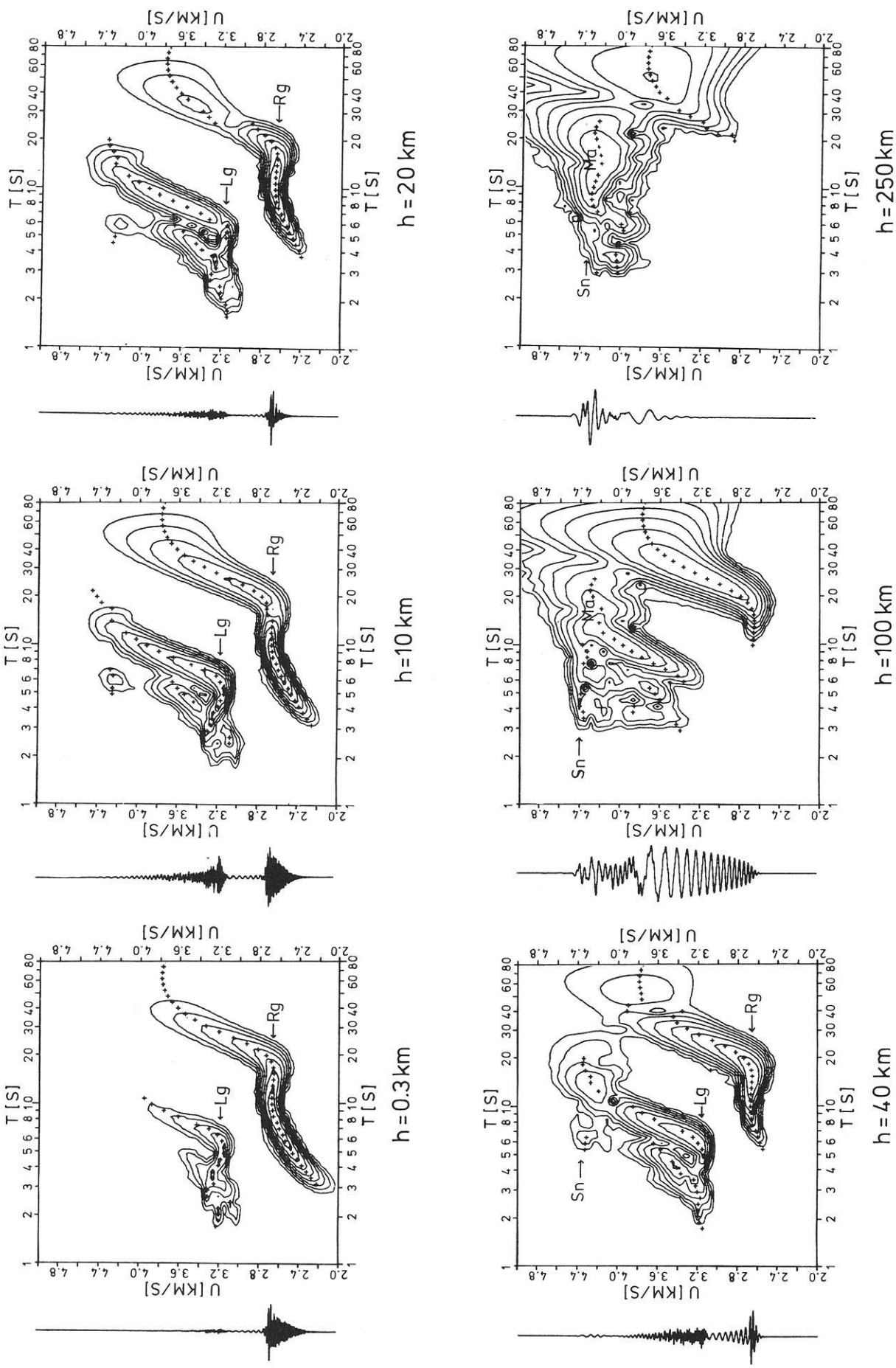

Fig. 4. Depth dependence of the excitation of Rayleigh waves for a vertical strike-slip source ($\lambda = 0°$, $\delta = 90°$, $\Theta = 45°$) and an Aki spectrum ($M_s = 6$)

modes show much greater amplitudes than the dispersed fundamental mode.

In Fig. 4 characteristic nodes in the Rayleigh wave excitation of the dislocation source can be observed. The corresponding periods also increase with source depth. For the vertical strike-slip source a minimum of the fundamental mode is found at 16 s for 10 km, at 25 s for 20 km and at 40 s for 40 km depth.

Source Spectrum

The source spectrum directly influences the generation of Rayleigh waves within the period range defined by the source depth. For the shallowest events (0.3 km) the source spectrum alone is responsible for the differences observed in Figs. 3 and 4.

In Fig. 5 the four different source spectra shown in Fig. 1 have been used for a vertical strike-slip source at 10 km depth. According to the higher-frequency spectral maximum of the lower magnitude earthquakes the excitation of the long-period part of the fundamental mode decreases and the *Lg*/*Rg* ratio consequently increases with decreasing magnitude. But even the highest-frequency earthquake spectrum ($M_s=4$) generates more long-period Rayleigh waves than the low-frequency explosion equivalent MM-spectrum for $Y=1$ Mt. For smaller yields the spectra would be shifted to even higher frequencies.

Source Type and Orientation

For a given source depth and source spectrum, an explosion point source with a spherical radiation pattern gives the maximum Rayleigh wave excitation. A buried dislocation source causes minima in the excitation depending on the orientation of the fault-plane, the observation angle, the source depth and the mode number. These minima are due to nodes in the radiation pattern of Rayleigh waves. Therefore the shape of the observed spectrum can be used for depth-estimation if the orientation of the fault-plane is known (Tsai and Aki, 1970). The reduction of amplitudes outside the minima decreases with increasing distance. Because of the superposition of higher modes a node in the excitation of the higher mode Rayleigh waves causes a smaller reduction in amplitudes than a node in the fundamental mode. Therefore the *Lg*/*Rg* ratio increases if the *Rg* amplitude is reduced by a minimum.

Five strike-slip sources (Fig. 6) and five dip-slip sources (Fig. 7) with dip-angles between 0° and 90° and an identical observation angle of $\Theta=30°$ are investigated for a source depth of 10 km and an Aki-spectrum of $M_s=6$. The maximum excitation of Rayleigh waves – indicated by the highest fundamental mode/higher mode ratio in Figs. 6 and 7 – is observed only for a dip-angle of 0° in both cases and for $\delta=90°$ in the dip-slip case. For the other dip-angles the amplitudes of the fundamental mode are reduced (however only slightly for $\delta=22.5°$ and $\delta=45°$ in the strike-slip case). Nodes are observed at 16 s in case of a vertical strike-slip and at 30 s in case of a dip-slip source with $\delta=45°$.

Summarizing the results of the model studies shown in Figs. 3 to 7 it seems possible to distinguish between shallow and deep and to a lesser degree between high-frequency and low-frequency sources by the analysis of real broad-band Rayleigh waves. An estimation of the fault-plane orientation in the case of a dislocation source requires data from more than one station.

Frequency-Time Analysis of Real Broad-Band Rayleigh Waves

When we consider real seismograms there are two major differences in comparison to the computational results which have to be considered: a) the existence of seismic noise and b) travel paths effects corresponding to different epicenters and lateral inhomogeneities. To avoid the first problem in initial investigations, strong events with high signal/noise ratio in the medium-period band can be used. To detect and analyse Rayleigh waves of smaller events also, array techniques such as frequency-wavenumber filtering and stacking methods can be applied. The second difficulty can be reduced by restricting the investigations to a relatively homogeneous region like the Eurasian continent (or parts of it) in case of the GRF-array.

In Fig. 8 the Rayleigh waves of three nuclear explosions from different parts of the USSR are analysed. The frequency-time structure of the Novaya Zemlya event and the Eastern Kazakh event are quite similar regarding the periods of major maxima. The dominating maxima belong to the *Rg* and *Lg* phases. The amplitude ratio is about 1 in both cases. This is equivalent to the theoretical results for an explosion source at 300 m depth in Fig. 3. The synthetic example of Fig. 3 is directly comparable to the Novaya Zemlya as the velocity model used represents the travel path Novaya Zemlya – GRF.

The periods corresponding to *Rg* (upper 6-db-contour-line) are located between 6 s and 10 s (Eastern Kazakh: second peak at 14 s) and those corresponding to *Lg* between 2 s and 6 s. The mean group velocities of both phases and the shape of the observed dispersion curves differ due to the different structures of the travel paths (higher velocities and a greater average depth of the Moho for the path Eastern Kazakh – GRF).

In contrast to these two underground explosions, which were contained in hard rock (presumably weapon tests), the Western Kazakh event represents one of the so-called 'peaceful' nuclear explosions (PNE) which are usually conducted for construction purposes. PNE events near the Caspian Sea in general generate less surface waves than the other explosions. The spectral content is also different as is revealed by a smaller *Lg*/*Rg* ratio and a shifting of the *Rg* phase towards longer periods (6-db-contour-line from 8.5 s to 15 s). Also the *P* arrival shows a relatively low-frequency spectrum. A lower-frequency source spectrum and/or a strong attenuation of high frequencies in unconsolidated sediments near the source would explain this effect.

Figure 9 shows the frequency-time analysis of four Central Asian earthquakes at different source depths. The Tadzikh event at 20 km depth generates mainly *Rg* and *Lg* phases within a period range from 9–18 s (*Rg*) and 5–6 s (*Lg*).

The average values for each phase are therefore of longer periods than the Novaya Zemlya and Eastern Kazakh events. The *Rg* maximum includes two parts at different group velocities. Additionally a maximum representing the *Ma* phase (11–18 s) and another stationary phase at 4.1 km/s, probably due to *Li* or a converted *Sn* phase, are situated in the upper part of the diagram.

An Eastern Kazakh earthquake at 40 km depth still generates strong *Rg* and *Lg* phases which are shifted to longer periods compared to the shallow event. The 6-db-contours of these maxima are found in the ranges 11–26 s (*Rg*) and

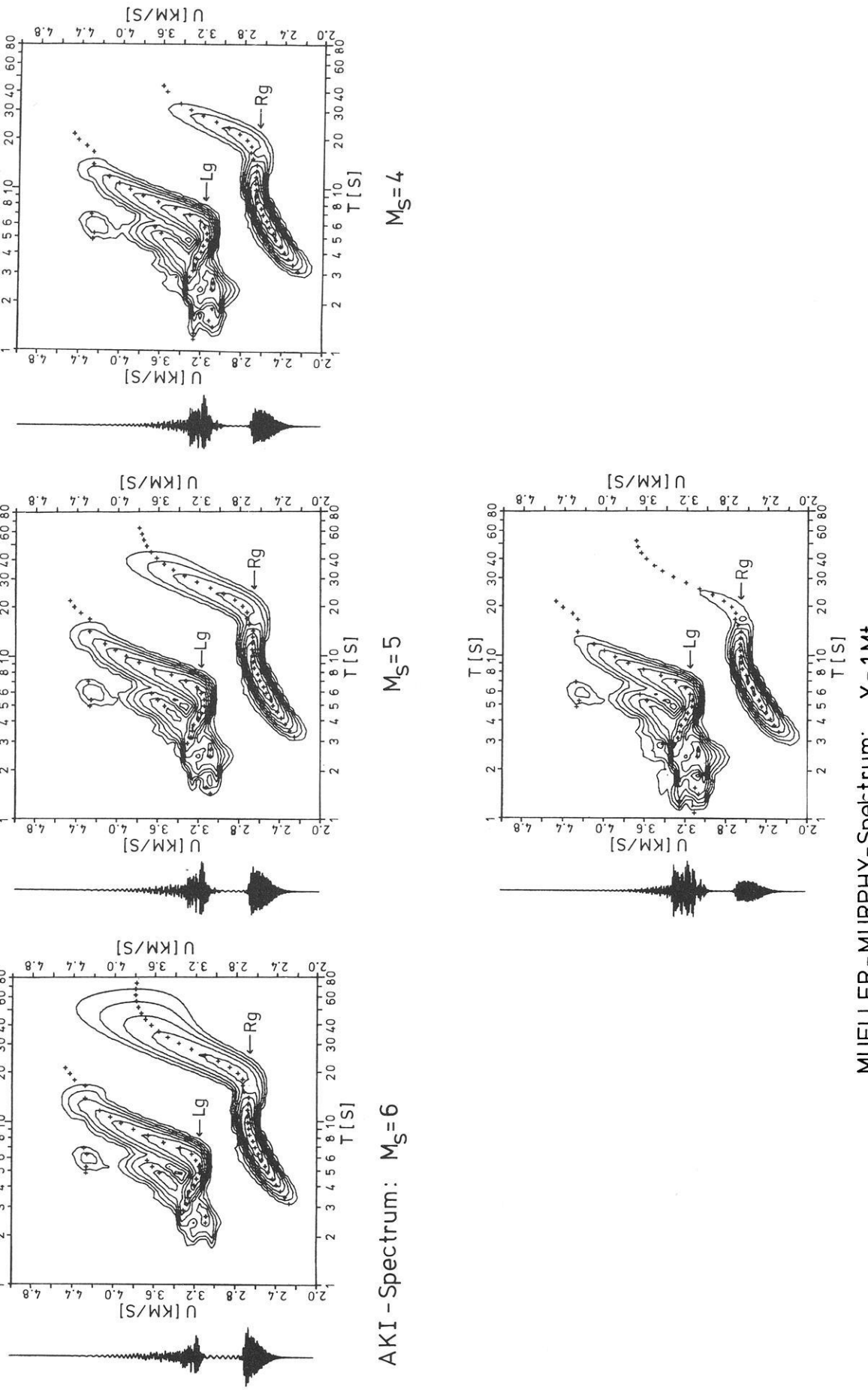

Fig. 5. Dependence of the Rayleigh wave excitation on the source spectrum for a vertical strike-slip source at 10 km depth

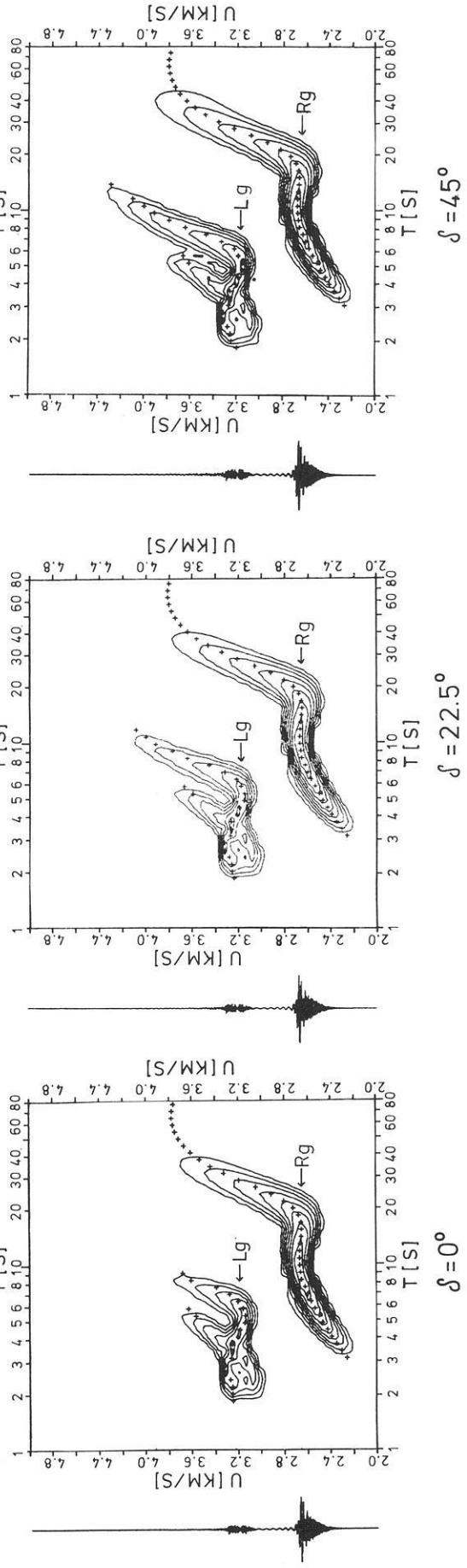

Fig. 6. Dependence of the Rayleigh wave excitation on dip-angle variations for a strike-slip source ($h = 10$ km)

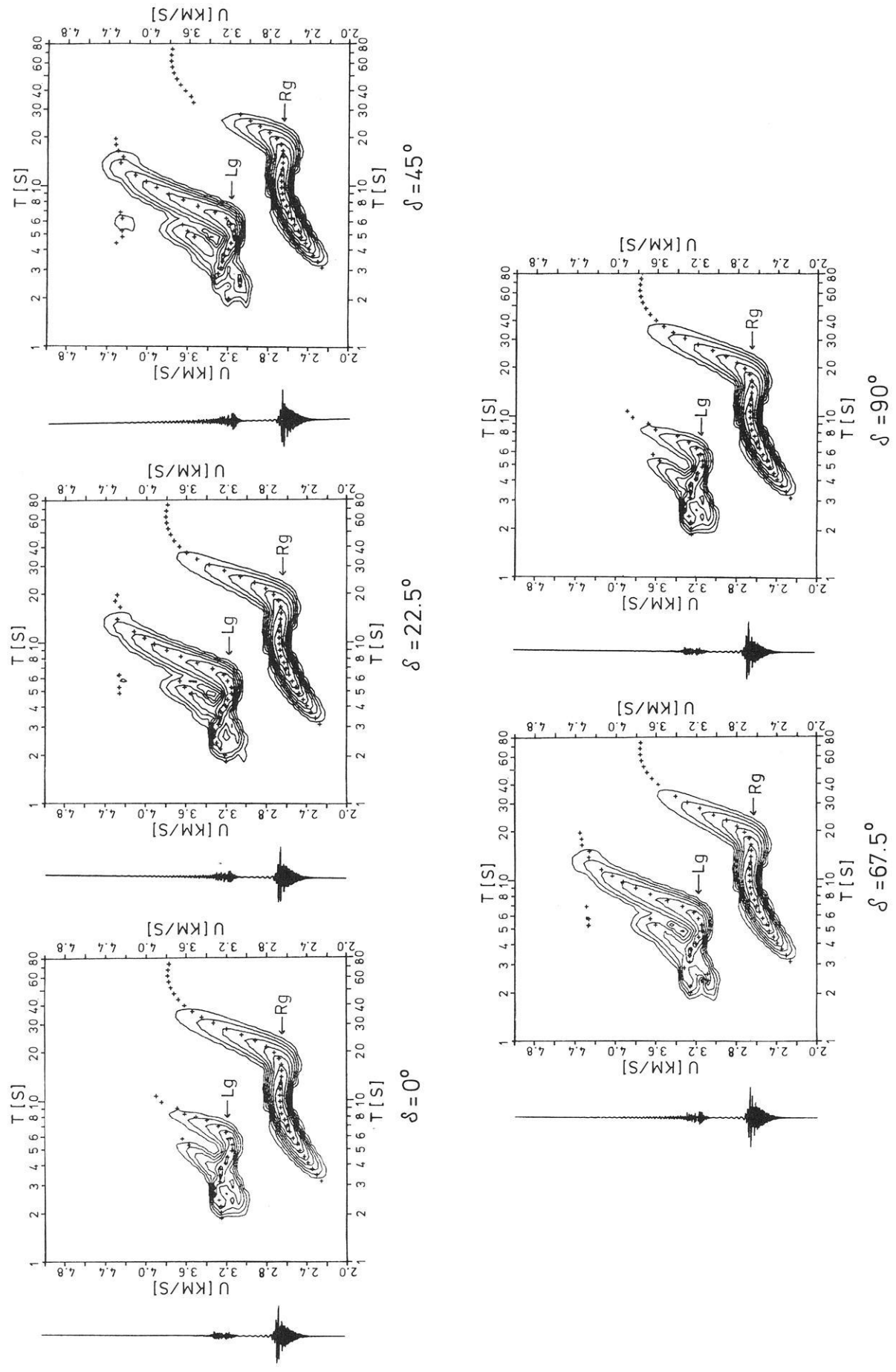

Fig. 7. Dependence of the Rayleigh wave excitation on dip-angle variations for a dip-slip source ($h = 10$ km)

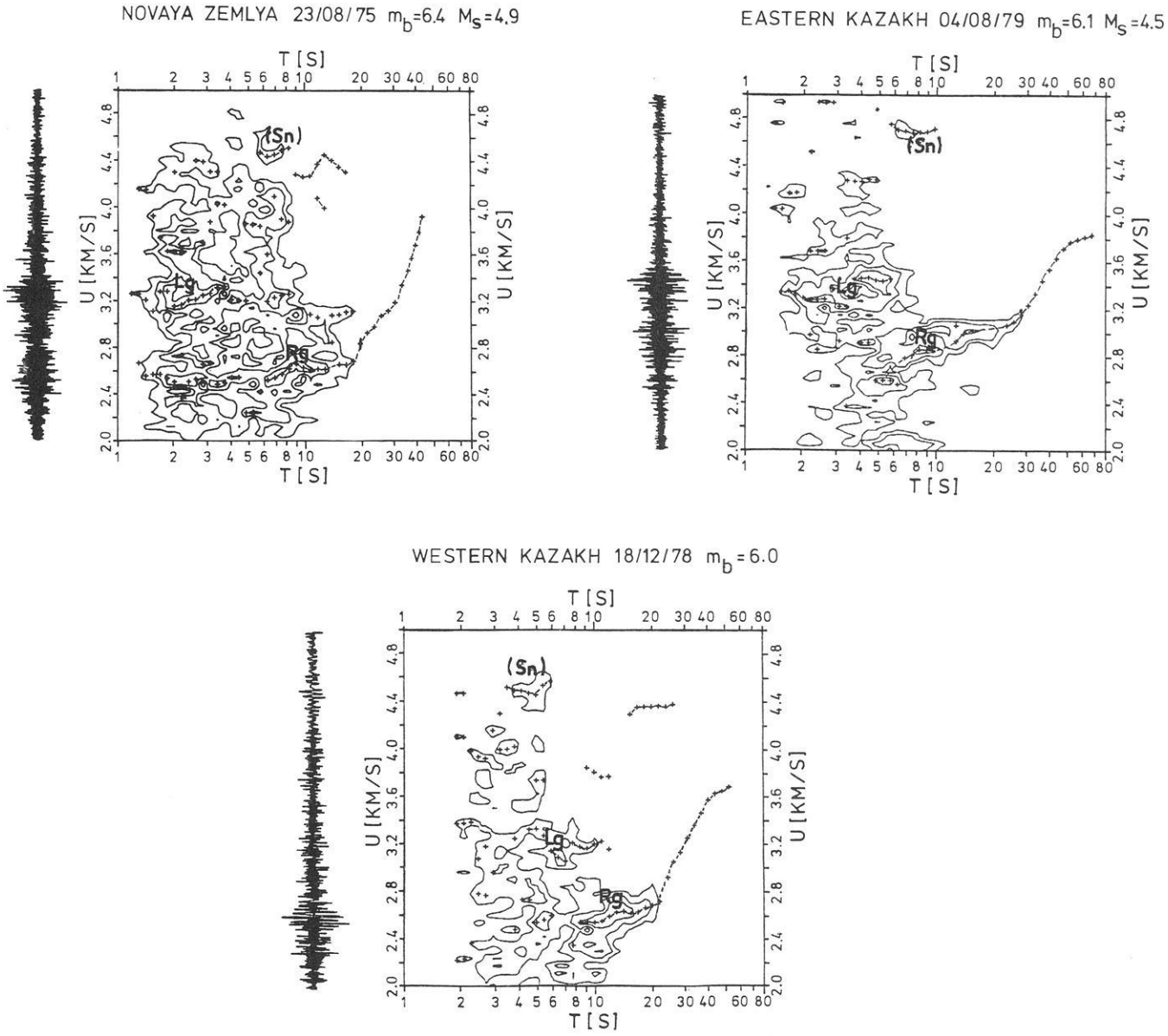

Fig. 8. Frequency-time analysis (upper 18 db) of broad-band, vertical component Rayleigh waves generated by three typical nuclear explosions from different sites in the USSR

5.4–8.3 s (*Lg*). Weak *Sn* and *Ma* phases are also excited. The dispersion curves of the fundamental mode and the group velocities of *Lg* for the explosion and the earthquake from Eastern Kazakh are almost identical due to the similar travel path.

Due to weak excitation of surface waves and therefore a smaller signal/noise ratio the Rayleigh waves of the Hindukush event ($h=99$ km) and the deep earthquake from the USSR-Afghanistan border region ($h=227$ km) are disturbed by seismic noise below 10 s. At 99 km depth an *Rg* phase but no *Lg* phase is observed. The strongly dispersive parts of the fundamental and first higher Rayleigh mode, which are also seen in the synthetic example in Fig. 4, are observed between 20 s and 70 s and between 8 s and 12 s respectively. The *Sn* and *Ma* phases are stronger and the *Ma* maximum is shifted towards longer periods (15–27 s) compared with shallower sources.

Sn and *Ma* dominate for the 227 km deep source. In this case the *Ma* maximum is located around 30 s and the fundamental mode can only be recognized around 20 s and between 60 s and 70 s. Crustal phases are not observed. The group velocity minimum corresponding to *Ma* shows the same value for the two events (4.3 km/s), but the *Sn* maximum of the Hindukush event arrives at a lower velocity (4.45 km/s) than the maximum of the event from the USSR-Afghanistan border region (4.6 km/s).

The examples shown in this section demonstrate that computed and observed seismograms are also comparable in fine structure in the medium-period band. The observed differences pertaining to a) the excitation of mantle phases by near surface sources and of crustal phases by deeper sources, b) differences in group velocities of equivalent phases, c) multiple arrivals and d) a diminishing coda – all not predicted by theoretical results – show that not all effects have been taken into account in the model computations. The differences are basically due to lateral inhomogeneities which cause multipathing, mode conversion and scattering. Also variable attenuation in the upper mantle

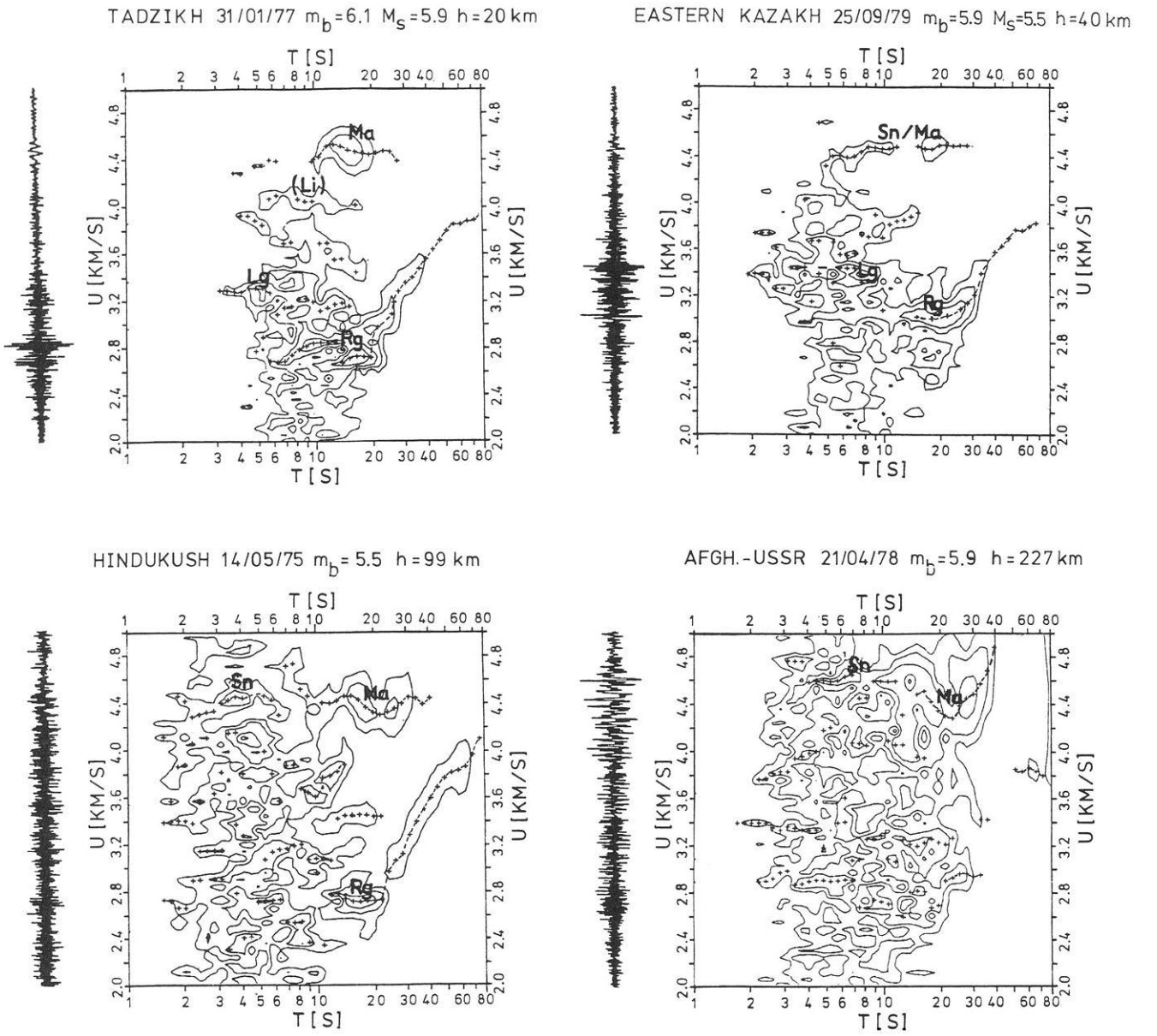

Fig. 9. Frequency-time analysis (upper 18 db) of broad-band, vertical component Rayleigh waves generated by four Central Asian earthquakes at different depths

which cannot be represented by an average model should be considered.

Quantification of Differences in Rayleigh Wave Excitation Caused by Different Sources

The differences in the frequency-time diagrams of synthetic Rayleigh waves excited by explosion and dislocation point sources at various depths are confirmed by the analysis of broad-band recorded Rayleigh waves and provide a starting point for establishing additional seismic discrimination parameters based on surface wave analysis.

A possible quantification scheme of the observed differences is the determination of maximum amplitudes in four different windows in the frequency-time domain which are shown in Fig. 10. Window 1 contains the observed variations in the location of *Rg* for travel paths over the Eurasian continent, window 2 the same for *Lg*, window 3 for the long-period part of *Sn* and *Ma* and window 4 for the long-period and dispersive part of the fundamental mode Rayleigh waves (named hereafter R_{LP}). The short- and medium-period part of *Sn* ($T<10$ s) is not used in this quantification scheme because the signal/noise ratio for shallow sources is usually very low. Using adequate filters or stacking methods for noise reduction the window 3 could be extended down to 1 or 2 s.

In case of real seismograms the amplitudes of the frequency-time matrix representing the ground velocity are corrected for each period by a representative 'noise'-amplitude determined just before the *Sn*-arrival (usually between 5.35 and 4.95 km/s) to reduce the influence of the signal-generated and the normal ground noise. The correction factor consists of the mean amplitude within the group velocity interval to which the standard deviation is added. The obtained maximum amplitudes A_1–A_4 are additionally multiplied by a weighting factor depending on the relative loca-

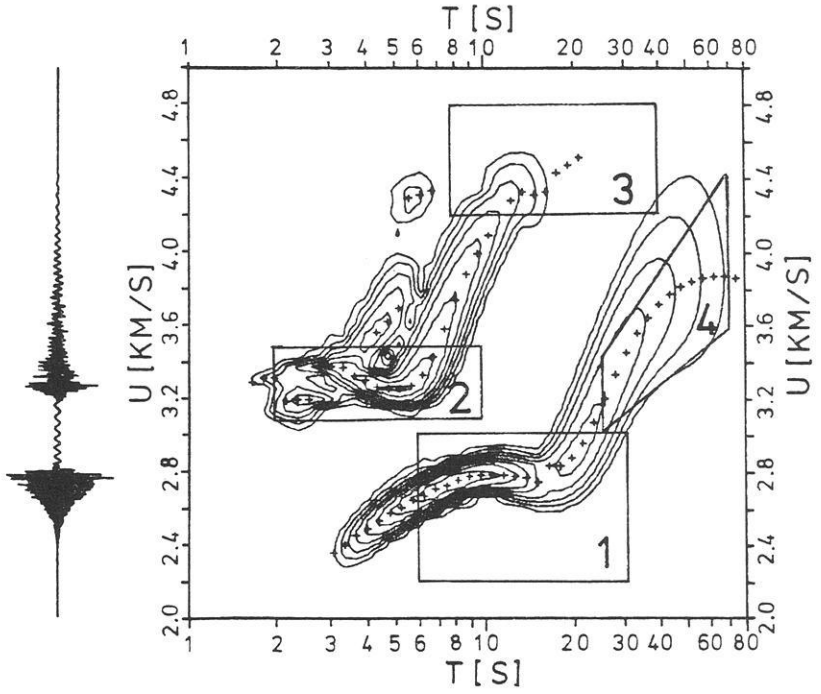

Fig. 10. Frequency-time windows for the quantification of Rayleigh wave excitation

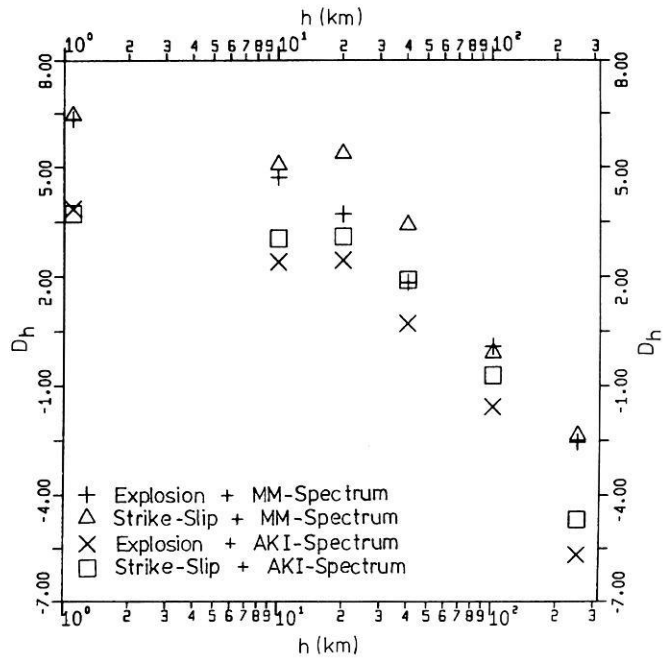

Fig. 11. Depth dependence of the D_h-discriminant based on synthetic Rayleigh wave seismograms

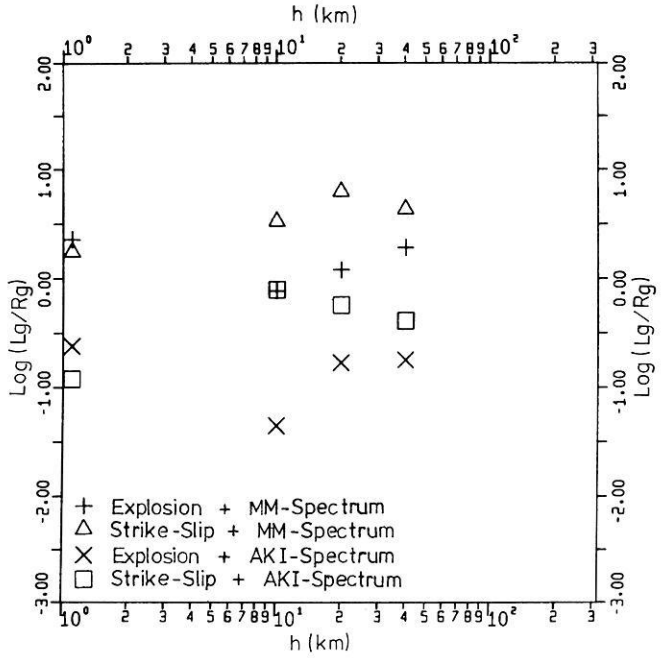

Fig. 12. D_s-discriminant versus depth based on synthetic Rayleigh wave seismograms

tion of the maximum according to the defined period interval.

For the comparison of different events, amplitudes or amplitude ratios or their combination can be used. A possible combination of amplitude ratios, mainly relevant to the influence of the source depth on the excitation of Rayleigh waves, is defined by

$$D_h = \log (A_1^+/A_4^-) + \log (A_2^+/A_3^-).$$

The two amplitude ratios should increase with decreasing source depth because the crustal phases *Rg* (A_1) and *Lg* (A_2) are strengthened while the subcrustal phases *Sn* and *Ma* (A_3) and R_{LP} (A_4) become smaller. This effect is enhanced by an opposite weighting of the numerator and denominator amplitudes (indicated by + and − signs).

The D_h-values are determined for the synthetic Rayleigh wave seismograms for the four combinations of explosion and strike-slip sources and MM- ($Y=1$ Mt) and Aki-source spectra ($M_s=6$) and the result is shown for the different source depths in Fig. 11. Except for a depth of 20 km, the D_h-values in all cases decrease steadily with increasing depth. Therefore a rough depth estimation should be possi-

Table 1a. Epicenter data from 20 nuclear explosions (USGS), azimuth and distance with respect to GRF

Nr.	Code	Date	Origin time	Coordinates	Magnitude		Distance (°)	Azimuth (°)	Region
					m_b	M_s			
1	N1	23/08/1975	08:59:57.9	73.369 N 54.641 E	6.4	4.9	30.2	23.2	Novaya Zemlya
2	N2	10/08/1978	07:59:57.7	73.336 N 54.792 E	5.9	4.3	30.2	23.3	Novaya Zemlya
3	N3	27/09/1978	02:04:58.2	73.380 N 54.669 E	5.6	4.5	30.2	23.1	Novaya Zemlya
4	N4	18/10/1979	07:09:58.3	73.338 N 54.807 E	5.8		30.2	23.2	Novaya Zemlya
5	N5	11/10/1980	07:09:57.0	73.313 N 55.021 E	5.7	3.8	30.3	23.4	Novaya Zemlya
6	E1	29/05/1977	02:56:57.8	49.944 N 78.846 E	5.6	5.0	42.3	62.7	Eastern Kazakh
7	E2	29/07/1977	03:06:58.0	50.034 N 78.927 E	5.3	5.2	42.3	62.5	Eastern Kazakh
8	E3	30/11/1977	04:06:57.5	49.957 N 78.931 E	5.9	3.5	42.3	62.6	Eastern Kazakh
9	E4	29/08/1978	02:37:06.5	50.008 N 78.996 E	5.9	4.0	42.3	62.5	Eastern Kazakh
10	E5	29/11/1978	04:33:02.9	49.956 N 78.765 E	6.0	4.3	42.2	62.7	Eastern Kazakh
11	E6	23/06/1979	02:56:57.6	49.918 N 78.915 E	6.3	4.4	42.3	62.7	Eastern Kazakh
12	E7	07/07/1979	03:46:57.4	50.053 N 79.965 E	5.8		42.3	62.4	Eastern Kazakh
13	E8	04/08/1979	03:56:57.2	49.901 N 78.959 E	6.1	4.5	42.3	62.7	Eastern Kazakh
14	E9	18/08/1979	02:51:57.3	49.971 N 79.010 E	6.1	4.1	42.3	62.6	Eastern Kazakh
15	U1	17/10/1978	13:59:57.8	63.143 N 63.392 E	5.5		30.9	44.4	Ural mountains
16	W1	17/10/1978	04:59:56.5	47.818 N 48.114 E	5.8	4.6	24.2	80.2	Western Kazakh
17	W2	18/12/1978	07:59:56.3	47.787 N 48.192 E	6.0		24.3	80.2	Western Kazakh
18	W3	17/01/1979	07:59:55.7	47.883 N 48.128 E	6.0		24.2	80.0	Western Kazakh
19	W4	14/07/1979	04:59:55.1	47.813 N 48.097 E	5.6		24.2	80.2	Western Kazakh
20	S1	04/10/1979	15:59:57.9	60.677 N 71.501 E	5.4		34.9	48.4	Western Siberia

Table 1b. Epicenter data from 20 earthquakes (USGS), azimuth and distance with respect to GRF

Nr.	Code	Date	Origin time	Coordinates	Depth (km)	Magnitude		Distance (°)	Azimuth (°)	Region
						m_b	M_s			
1	F1	13/07/1977	08:09:15.7	29.880 N 67.454 E	10	5.1	5.5	46.3	93.6	Western Pakistan
2	F2	02/01/1978	06:31:27.5	41.540 N 44.244 E	10	5.3	5.1	24.3	96.9	Western Caucasus
3	F3	06/04/1979	18:30:06.4	41.900 N 77.545 E	19	5.2	4.9	45.5	73.4	Kirgiz-Sinkiang border region
4	F4	22/12/1980	12:51:17.6	34.350 N 50.403 E	18	5.2	5.2	32.5	103.2	Iran
5	M1	19/05/1975	19:47:44.8	35.160 N 80.801 E	26	5.5	5.1	51.6	78.6	Kashmir-Tibet border region
6	M2	01/04/1976	04:31:16.7	51.115 N 97.962 E	33	5.2	4.7	52.1	52.8	USSR-Mongolia border region
7	M3	03/08/1976	07:50:19.8	40.797 N 77.876 E	33	5.2	5.2	46.3	74.5	Kirgiz-Sinkiang border region
8	M4	03/09/1976	21:52:46.8	38.924 N 70.716 E	43	5.1	4.7	42.9	81.1	Afghanistan-USSR border region
9	M5	05/09/1976	22:07:34.9	38.298 N 40.853 E	22	5.1	4.8	24.0	107.0	Turkey
10	M6	03/06/1977	01:05:23.7	39.874 N 71.786 E	24	5.1	5.0	43.0	79.3	Tadzikh
11	M7	25/12/1977	16:18:54.7	38.923 N 70.796 E	33	5.3	4.7	42.9	81.0	Afghanistan-USSR border region
12	M8	25/09/1979	13:05:53.6	45.083 N 77.006 E	40	5.9	5.5	43.5	69.8	Eastern Kazakh
13	I1	14/05/1975	22:23:02.8	36.082 N 70.894 E	99	5.5		44.6	84.3	Hindukush
14	I2	08/10/1978	14:20:05.6	39.389 N 74.718 E	62	5.8		45.2	78.0	Southern Sinkiang
15	I3	13/20/1979	22:09:29.6	36.517 N 76.892 E	63	6.1		48.2	79.8	Kashmir-Sinkiang border region
16	T1	27/11/1976	21:42:12.2	36.507 N 71.042 E	190	6.1		44.5	83.7	Afghanistan-USSR border region
17	T2	03/06/1977	02:31:04.7	36.436 N 70.762 E	210	5.5		44.3	84.0	Hindukush
18	T3	21/04/1978	15:22:57.6	36.620 N 71.274 E	227	5.9		44.6	83.4	Afghanistan-USSR border region
19	T4	23/10/1978	08:07:31.6	36.483 N 70.964 E	185	5.6		44.4	83.8	Afghanistan-USSR border region
20	T5	26/60/1979	03:04:51.8	36.475 N 71.218 E	229	5.7		44.6	83.6	Afghanistan-USSR border region

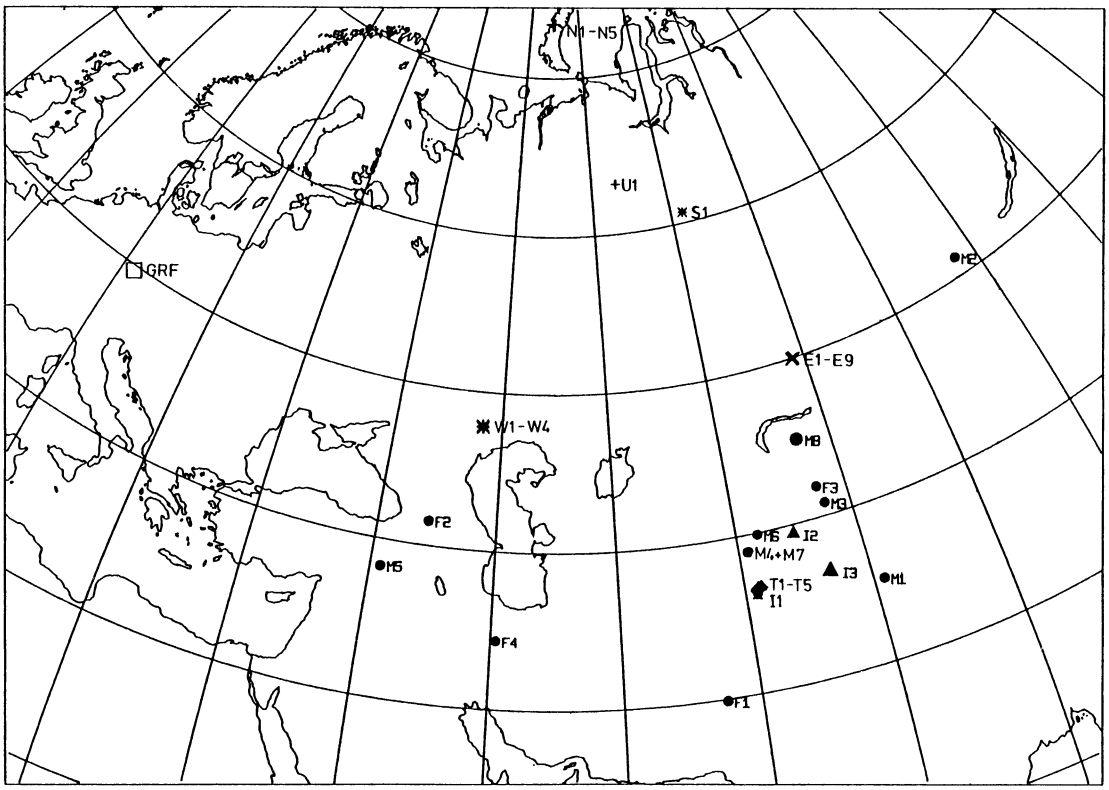

Fig. 13. Location of epicenters for the 20 nuclear explosions (*crosses and stars*) and the 20 earthquakes (*solid circles, triangles and squares*) used for discrimination

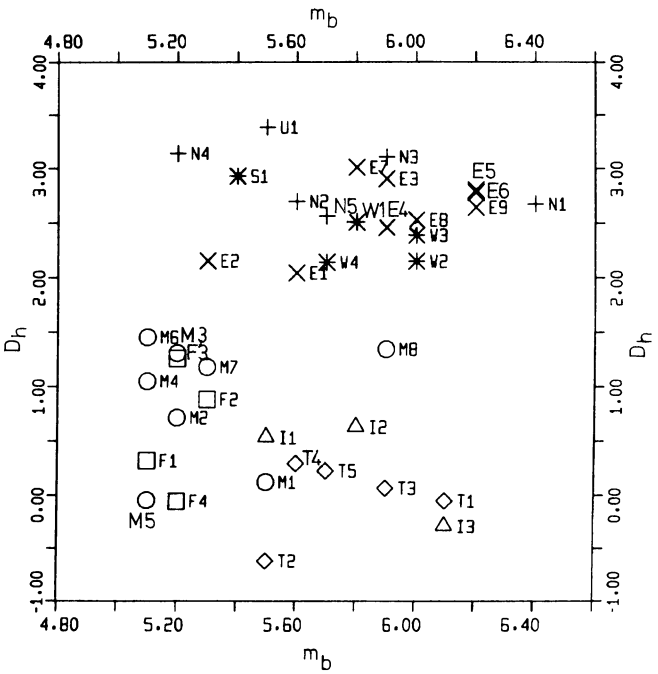

Fig. 14. D_h-values versus m_b for a group of explosions (*crosses and stars*) and group of arthquakes (*circles, triangles and squares*)

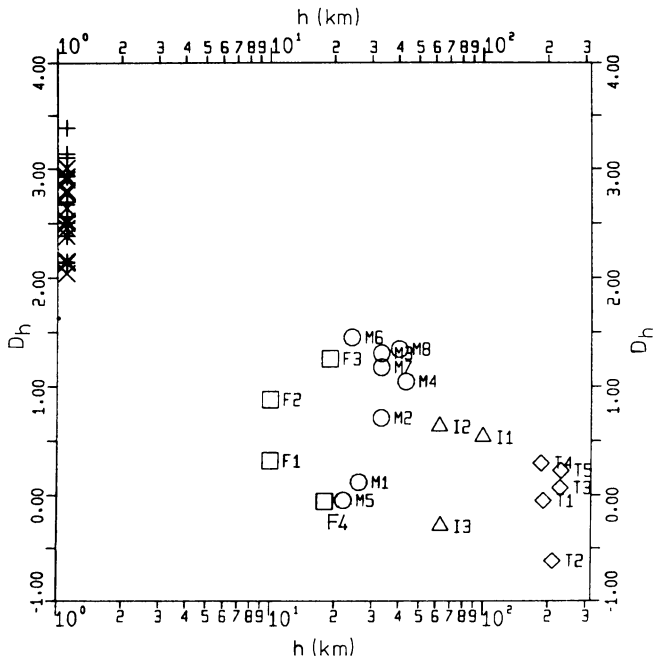

Fig. 15. D_h-values versus depth for a group of explosions (*crosses and stars*) and a group of earthquakes (*circles, triangles and squares*)

ble by using this discriminant. In particular, a discrimination of high-frequency shallow sources and arbitrary deeper sources is suggested by this investigation.

Another discrimination parameter, mainly relevant to the influence of the source spectrum on the excitation of Rayleigh waves is represented by the Lg/Rg ratio. Assuming that the excitation of Lg and Rg takes place in the same parts of the earth's crust the observed relative differences in the Lg and Rg amplitudes are dependent on the different amplitude-depth functions and on the relative amplitudes of the source spectrum at the different periods.

Therefore the usefulness of a discriminant defined by

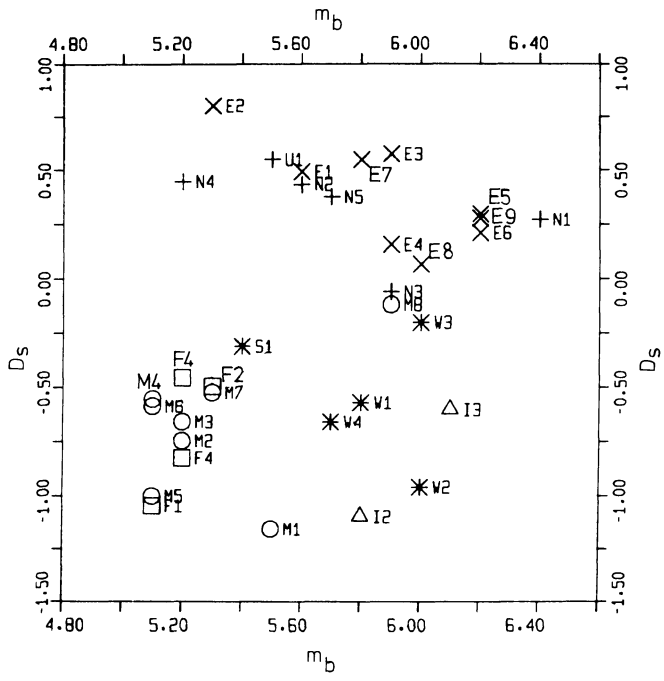

Fig. 16. D_s-values versus m_b for a group of explosions (*crosses and stars*) and a group of earthquakes (*circles, triangles and squares*)

$$D_s = \log (A_2^+ / A_1^-)$$

should first be evaluated using the synthetic Rayleigh wave seismograms. The results are shown in Fig. 12 where the theoretical D_s-values are plotted versus h for source depths down to 40 km. A clear difference between the high-frequency and low-frequency source spectrum is observed for the same source mechanism at each depth. But due to nodes in the excitation of the fundamental mode in the case of dislocation sources, an overlap of the D_s-values for the explosion and strike-slip sources occurs for 10 km depth. Therefore a general discrimination of high-frequency and low-frequency sources without regard to the source mechanism and the source depth is not possible. Nevertheless the essential discrimination problem, namely the separation of highfrequency sources at shallow depth from low-frequency sources at arbitrary depth, can be solved at least in terms of model computations.

Application of Discriminants to Real Broad-Band Data

For two sets each of 20 nuclear explosions and earthquakes located in the USSR and adjacent areas (see Table 1 for epicenter data) the two discriminants are applied. The locations of the epicenters in relation to the GRF-array are shown in Fig. 13. The explosion set consists of events from Novaya Zemlya (5 events), Eastern Kazakh (9), Western Kazakh (4), Ural mountains (1) and Western Siberia (1). The body wave magnitude ranges from 5.3 to 6.4. The shallow (4) and normal deep earthquakes (8) from Western and Central Asia were selected for their intermediate m_b-values ($5.0 < m_b \leqq 5.5$) with the exception of event M8 (Eastern Kazakh event of Fig. 9 with $m_b = 5.9$). Due to a lower absolute excitation of surface waves by deeper sources the m_b-values of the selected intermediate (3) and deep earthquakes (5) from the Afghanistan-USSR border region are slightly greater ($5.5 \leqq m_b \leqq 6.1$).

In Fig. 14 the discrimination potential of the D_h-discriminant is demonstrated by a plot of D_h versus m_b. Explosions (cross and star symbols) and earthquakes (other symbols) are completely separated. Also the PNE-events W1–W4, S1 and (presumably) U1 are classified as explosions by the D_h-discriminant although the frequency-time structure of the transient signal is different from that of the other explosions.

Additionally the depth dependence of the values can be seen from Fig. 15. Here a decrease of D_h-values with increasing depth can be well discerned. In comparison to theoretical investigations (Fig. 11) the decay of D_h-values is much smaller and the variance much higher than predicted. In particular, shallow and deep sources, respectively, produce too high and too low values. This is explained by the presence of relatively high noise amplitudes, which prohibits the tracing of a decreasing phase.

In Fig. 16 the D_s-discriminant is applied to all events which are not deeper than 70 km because deeper events do not generate significant *Lg* and *Rg* amplitudes. Apart from the PNE events (W1–W4 and S1) the two groups are also separated although the D_s-values of events N3 and M8 are very close. As demonstrated in Fig. 9 the PNE events near the Caspian Sea show a spectral content different from that of the other nuclear explosions. This results in a low *Lg*/*Rg* ratio, and therefore the five PNE events are misclassified and located within the earthquake population.

Discussion and Conclusions

Theoretical seismograms provide a useful tool for the prediction and interpretation of differences in the Rayleigh wave excitation of various earthquake and explosions sources. These differences are mainly due to changes in source parameters, namely a) source depth, b) source spectrum and c) source type and orientation. The model computations were carried out for a simple horizontally layered earth model. Additional travel paths effects observed in real broad-band data, such as differences in group velocities, multiple arrivals, mode conversion and in the duration of the coda are caused by lateral inhomogeneities. They are therefore not considered in the model computations.

A detailed frequency-time analysis of the calculated seismograms and a comparison with real braod-band Rayleigh wave seismograms show the existence of the fundamental and higher mode stationary phases *Rg*, *Lg* and *Sn* in the medium-period band between 2 s and 20 s and also of the main part of *Ma* and the dispersed part of the fundamental mode in the long-period band above 20 s. The model computations do not include the high-frequency band above 0.75 Hz. One reason for this is the limited computer time, another that for teleseismic distances Rayleigh wave seismograms recorded at GRF do not show a significant signal content below 2 s.

A quantification of the Rayleigh wave excitation using the maximum amplitudes within four frequency-time windows representing the *Rg*, *Lg*, *Sn-Ma* and R_{LP} leads to parameters which give a rough idea about the source depth and the source spectrum. These parameters consist of amplitude ratios – or of a combination of these – and are therefore independent of the absolute value of the ground motions. The D_h-discriminant (combination of *Lg*/

Ma and Rg/R_{LP}) is basically sensitive to the source depth and allows the separation of high-frequency shallow from arbitrary deeper sources and a rough depth estimation for earthquakes. On the other hand the D_s-discriminant (Lg/Rg ratio) depends mainly on the source spectrum and allows discrimination between high-frequency shallow sources and low-frequency sources for depths down to approximately 70 km.

The application of these discriminants to two sets of broad-band recorded earthquakes and explosions gives promissing results. Only 'peaceful' nuclear explosions near the Caspian Sea and in Western Siberia were misclassified by the D_s-discriminant.

The events used in this study are, however, quite strong and the application of our discriminants to smaller events has to be further investigated. Array techniques like frequency-wavenumber filtering and stacking methods would improve the signal/noise ratio in the medium-period band by a reduction of the microseismic noise. Looking also at regional events ($\Delta < 20°$) the adopted frequency-time windows should, because of the higher-frequency signal content, be expanded to higher frequencies to include even higher modes in the analysis.

Acknowledgements. The author wishes to thank Prof. H.-P. Harjes for suggesting this work, for many useful discussions and a critical reading of the manuscript. He also thank R. Kind and D. Seidl for a broad support resulting in many suggestions, discussions and the provision of computer programs. He is grateful to B. Buttkus, P. Hubral and R. Kind for critically reading this manuscript. This work was supported by the Auswärtiges Amt (Foreign Office) and the GRF-array project by the Deutsche Forschungsgemeinschaft (German Research Council) and the Bundesanstalt für Geowissenschaften und Rohstoffe (Federal Institute for Geosciences and Natural Resources).

References

Aki, K.: Scaling law of seismic spectrum. J. Geophys. Res. **72**, 1217–1231, 1967

Anderson, D.L., Hart, R.S.: *Q* of the earth. J. Geophys. Res. **83**, 5869–5882, 1978

Calcagnile, G., Panza, G.F.: Vertical and *SV* component of *Sa*. Geophys. J.R. Astron. Soc. **38**, 317–325, 1974

Dziewonski, A., Bloch, S., Landisman, M.: A technique for the analysis of transient seismic signals. Bull. Seismol. Soc. Am. **59**, 427–444, 1969

Gupta, I.N., Barker, B.W., Burnetti, J.A., Der, Z.A.: A study of regional phases from earthquakes and explosions in Western Russia. Bull. Seismol. Soc. Am. **70**, 851–872, 1980

Gupta, I.N., Burnetti, J.A.: An investigation of discriminants for events in Western USSR based on regional phases recorded at station Kabul. Bull. Seismol. Soc. Am. **71**, 263–273, 1981

Harjes, H.-P., Seidl, D.: Digital recording and analysis of broad-band seismic data at the Graefenberg (GRF)-Array. J. Geophys. **44**, 511–523, 1978

Kind, R.: The reflectivity method for a buried source. J. Geophys. **44**, 603–612, 1978

Kind, R.: Extensions of the reflectivity method. J. Geophys. **45**, 373–380, 1979

Knopoff, L., Schwab, F., Kausel, E.: Interpretation of *Lg*. Geophys. J.R. Astron. Soc. **33**, 389–404, 1973

Mantovani, E., Schwab, F., Liao, H., Knopoff, L.: Teleseismic *Sn*: a guided wave in the mantle. Geophys. J.R. Astron. Soc. **51**, 709–726, 1977

Mueller, R.A., Murphy, J.R.: Seismic characteristics of underground nuclear detonations. Part I: Seismic spectrum scaling. Bull. Seismol. Soc. Am. **61**, 1675–1692, 1971

Mykkeltveit, S., Husebye, E.S.: *Lg* propagation in Eurasia. In: Identification of seismic sources – earthquake or underground explosion, NATO Advanced Study Institutes Series, C.: Mathematical and Physical Sciences **74**. Dordrecht: Reidel 1981

Nakanishi, K.K., Schwab, F., Kausel, E.G.: Interpretation of *Sa* on a continental structure. Geophys. J.R. Astron. Soc. **47**, 211–223, 1976

Nuttli, O.W.: On the attenuation of *Lg* waves in Western and Central Asia and their use as a discriminant between earthquakes and explosions. Bull. Seismol. Soc. Am. **71**, 249–261, 1981

Panza, G.F., Calcagnile, G.: *Lg*, *Li* and *Rg* from Rayleigh modes. Geophys. J.R. Astron. Soc. **40**, 475–487, 1975

Schwab, F., Kausel, E., Knopoff, L.: Interpretation of *Sa* for a shield structure. Geophys. J.R. Astron. Soc. **36**, 737–742, 1974

Seidl, D.: Spezielle Probleme der Theorie seismischer Oberflächenwellen mit Beobachtungsbeispielen aus Europa. Dissertation, Universität Karlsruhe, 1971

Stephens, C., Isacks, B.L.: Towards an understanding of *Sn*: normal modes of Love waves in an oceanic structure. Bull. Seismol. Soc. Am. **67**, 69–78, 1977

Tsai, Y, Aki, K.: Precise focal depth determination from amplitude spectra fo surface waves. J. Geophys. Res. **75**, 5729–5743, 1970

Wielandt, E.: Astatic vertical pendulum supported by a leaf spring. J. Geophys. **41**, 545–546, 1975

Received June 28, 1982; Revised version September 6, 1982
Accepted September 8, 1982